Mapping and ablation of atrial tachyarrhythmias : from signal to substrate

Groot, N.M.S. de

chapter

4

Comparison of Epicardial Breakthrough of Fibrillation Waves between Patients with Acute and Chronic Atrial Fibrillation

Natasja MS de Groot

Richard M. Houben, Robert Klautz, Jerry Braun,
Joep LRM Smeets

Maurits A. Allessie, Martin J. Schalij

Abstract

Introduction: An epicardial breakthrough (EB) during atrial fibrillation (AF) is thought to be the result of transmural dissociation of fibrillatory waves. In this study, characteristics of EB during induced (AAF) and chronic AF (CAF) were compared and the impact of EB on conduction in the epicardial plane was examined.

Methods: Epicardial mapping during cardiac surgery (244 electrode-array, inter-electrode distance 2.25 mm) of the right atrial free wall was performed during AAF in patients (n = 20, age 31 ± 12 yrs.) with normal atria and no history of AF and during CAF in patients with valvular disease (n = 12, age 66 ± 9 yrs.). Episodes of 8 seconds of AF were analyzed. An EB was defined as a new wavefront arising within the mapping area which could not be explained by propagation of fibrillatory waves in the epicardial plane. The incidence and spatial distribution of EB was assessed. The degree of pre-excitation by each EB was measured and AF cycle length at EB- and non-EB sites were compared. At every EB origin, electrogram morphology was analyzed and the incidence of conduction block was measured.

Results: The incidence of EB during CAF was higher than during AAF (1.49 ± 0.82 [0.33-3.41]/beat versus 0.24 ± 0.25 [0-0.77]/beat, $p<0.001$). In all patients, EB were non-repetitive and randomly distributed. The majority of electrograms recorded at EB origins consisted of fractionated potentials (AAF: 64 ± 32%, CAF: 62 ± 18%) and fractionation was associated with shorter EB coupling intervals (AAF: $r = -0.14$, $p = 0.04$, CAF: $r = -0.10$, $p = 0.04$). Median AFCL (AAF: 157 ± 26 ms CAF: 185 ± 28 ms, $p<0.001$) were longer than
EB coupling intervals (AAF: 128 ± 27 ms, CAF: 171 ± 26 ms). Pre-excitation was higher in the CAF patients (56 ± 15 ms versus 38 ± 12 ms, $p = 0.03$) and conduction block at the EB origin occurred more often (AAF: 77 ± 11%, CAF: 86 ± 12%, $p = 0.03$).

Conclusions: During AF, EB frequently occur at the right atrial free wall. Comparing AAF and CAF patients, there was a higher incidence of EB during CAF. EB appear as solitary events scattered throughout the mapping area and they were preceded by a variety of fibrillation intervals. The findings of this study favors increased 3-dimensional conduction of fibrillatory waves during chronic human AF.

Introduction

Mapping of atrial fibrillation (AF) is usually performed on either the endocardial or the epicardial surface of the atria, assuming that atrial activation is mainly a two-dimensional process. However, several mapping studies have suggested that this assumption might be an oversimplification.[1-6]

Epicardial mapping of the right atrial free wall during induced AF in humans with non-dilated atria showed that most fibrillatory waves propagated in the epicardial plane, though incidentally wavefronts emerged 'de novo' in the middle of the mapping area (1.4 ± 2.5% of beats).[5] These *epicardial breakthroughs* were thought to be the result of transmural conduction of fibrillatory waves.

Experimental mapping studies confirmed the presence of three-dimensional conduction in the atria.[2-4] By simultaneously mapping of the endo- and epicardium in isolated canine atria, it was demonstrated that significant differences in timing of activation could exist between endo- and epicardium, demonstrating that these two layers were activated asynchronously. Asynchronous endocardial and epicardial activation particularly occurs in thicker parts of the atria like the pectinate muscles and it is enhanced at higher activation rates. It was also demonstrated that epicardial breakthrough observed during AF was actually the consequence of transmural conduction or reentry through pectinate muscle bundles connected to the epicardium.

In chapter 2, we have described that the incidence of epicardial breakthrough during chronic AF (CAF) in patients with valvular disease was significantly higher than the incidence of epicardial breakthroughs during induced AF (AAF) in patients with normal atria.

In the present study, we compared characteristics of epicardial breakthrough of fibrillatory waves between patients with AAF and CAF and studied its impact on the conduction of fibrillatory waves in the epicardial plane.

Methods

Study Population

Epicardial mapping during AAF was performed in patients (n = 20, 14 male, age 31 ± 12 yrs) during open chest surgery for interruption of an accessory pathway. All patients had normal sized atria (left atrial diameter 38 ± 6 mm) and no history of valvular or coronary artery disease. A more detailed description of this study population has been given previously.[5]

Epicardial mapping during CAF was performed in patients (n = 12, 7 male, age 66 ± 9 yrs) during cardiac surgery for valvular heart disease. All CAF patients had AF lasting for more than one year. Characteristics of CAF patients are summarized in Table 1.

Data Acquisition

In the AAF patients, AF was induced by programmed electrical stimulation through electrodes sutured to the right atrial appendage.

Epicardial mapping of the right atrium was performed using a spoon-shaped mapping array prior to cardiopulmonary bypass. This mapping array, – containing 244 unipolar electrodes (diameter: 0.3 mm, inter-electrode distance: 2.25 mm) was placed on the middle of the right atrial free wall, covering an area of 36x36 mm.

A silver electrode plate was placed inside the thoracic cavity to serve as indifferent electrode. A 256-channel computerized mapping system was used for simultaneously recording and processing of 244 unipolar fibrillation electrograms and a surface ECG (amplification: gain 1000, filtering: bandwidth 1-500 Hz, sampling rate: 1 KHz, analogue to digital conversion: 12 bits).

Data Analysis

Time windows of 8 seconds of AF – with exclusion of the first and last 12 seconds of an episode of induced AF – were off-line analyzed using specialized mapping software. Epicardial local activation times were automatically determined by marking the maximum negative derivative of unipolar fibrillation potentials. All markings were visually verified and edited if necessary. Fibrillation maps were constructed as previously described in chapter 2.

Fibrillation Intervals

At each electrode, the fibrillation intervals were determined by measuring the time between activation by consecutive fibrillatory waves. Median AF cycle length (AFCL) was calculated from all fibrillation intervals recorded by the 244 unipolar electrodes during 8 seconds of AF (AAF: n = 11,070 ± 3826, CAF: n = 5781 ± 2444).

Table 1. **Characteristics of the CAF patients**

pt no.	age	gender	valvular disease	AAD	LAD (mm)	LVEF (%)	AF duration	CVP (mmHg)
1	68	M	MVD	digoxin	69	37	> 2 yrs	15
2	68	M	MVD	digoxin	72	42	> 9 yrs	15
3	75	M	MVD	sotalol, digoxin	59	56	> 1 yr	NA
4	54	M	MVD	sotalol, digoxin	56	59	> 1 yr	8
5	69	F	MVD	verapamil + digoxin	47	35	> 5 yrs	16
6	55	F	MVD	–	70	64	> 6 yrs	10
7	67	F	MVD	sotalol, digoxin	49	66	> 1 yr	NA
8	76	F	MVD	sotalol, digoxin	60	64	> 2 yrs	20
9	66	F	AOD	sotalol, digoxin	62	59	> 1 yr	12
10	53	M	MVD	–	58	62	> 1 yr	8
11	58	M	MVD	sotalol			> 1 yr	NA
12	80	M	AOD	–	56	47	> 1 yr	5
mean/sd	66 ± 9				59 ± 8	54 ± 11		12 ± 5

M: male, F: female, MVD: mitral valve disease. AOD: aortic valve disease,
AAD: anti-arrhythmic drugs, LAD: left atrial diameter, LVEF: left ventricular ejection fraction, CVP = central venous pressure measured during cardiac surgery, NA: not available.

Conduction Velocity

Intra-atrial conduction velocity was determined by measuring local conduction vectors in surface areas of 2.25x2.25 mm. Because local conduction velocities were not distributed normally, the median value of all vectors (AAF: n = 9227 ± 2211, CAF: n = 5752 ± 28) was used to represent the conduction velocity of fibrillatory waves at the right atrial free wall.

Characteristics of Epicardial Breakthrough

Isochronal maps were used for identification of EB. An EB was defined as the emergence of a new wavefront in the mapping area which could not be explained by wavefronts traveling in the epicardial plane. A typical example of an EB is shown in figure 1 (t = 20 ms, left panel). Atrial tissue in the upper part of the mapping area is pre-excited by a radially spreading wavefront. Sites which were activated at least 5 ms before all surrounding electrodes which were a part of the expanding wavefront were labeled as the origin of EB.

The incidence of EB was defined as the number of EB per 'beat' in a mapping area of 3.6x3.6 cm. The median AFCL was used to calculate the number of beats occurring during 8 seconds of AF. To assess the spatial distribution of EB within the mapping area, distances between consecutive EB were measured.

The unipolar electrogram recorded at the EB origin was classified as a single, double or a fractionated potential. Single potentials consist of a single rapid negative deflection usually preceded by a positive deflection of varying amplitude. The R-S difference, defined as the difference in R and S amplitude divided by the total amplitude, was calculated for all single potentials.[7] When fibrillation potentials contain multiple deflections, only components with an amplitude of at least 25% of the amplitude of the largest deflection of the fibrillation potential were taken into account. A double potential was defined as a potential consisting of 2 consecutive negative deflections and potentials with more than 2 deflections were classified as fractionated potentials.

Impact of Epicardial Breakthrough on Conduction of Fibrillatory Waves

An EB can be the result of a premature activation originating from the endocardium or it can be the result of delayed excitation of the epicardium giving endocardial fibrillatory waves the opportunity to activate the epicardial layer. Therefore, the relation between the fibrillation interval preceding an EB (*EB coupling interval*) and the median AFCL was assessed. Also, the median AFCL of EB sites were compared with other parts of the mapping area.

The degree of pre-excitation was estimated for every EB. For this purpose, the earliest fibrillatory wave propagating towards the EB origin was identified (right panel Figure 1). In case of multiple wavelets, the fibrillatory wave closest to the EB origin was selected.

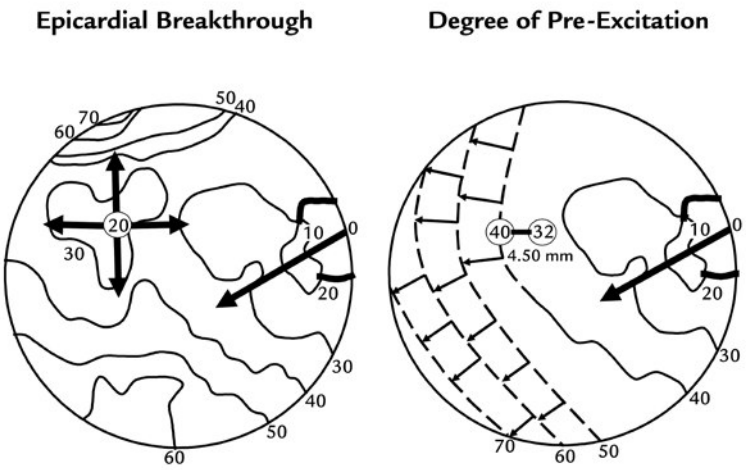

Figure 1.

Isochronal maps of the right atrial free wall; isochrones were drawn at 10 ms intervals, arrows indicate main activation direction and lines of conduction block are represented by thick black lines. Left: A new wavefront, expanding in all directions, arose from the upper left part of the mapping area. The origin of the EB is encircled. Right: dashed isochrones represent the assumed pattern of activation if there had not been an EB. The estimated degree of pre-excitation of the epicardial breakthrough was 20-40 = -20 ms.
See text for a more detailed explanation.

Then, the shortest distance from the site of earliest activation by the EB (local activation time: 20 ms) to the nearest electrode activated by the approaching fibrillatory wave was measured (local activation time 32 ms, distance 4.50 mm). Next, the expected activation time by the approaching epicardial fibrillatory wave at the site of EB if the EB would not have happened was determined. The expected activation time was calculated by summation of the activation time at the nearest electrode to the EB origin (32 ms) activated by the approaching fibrillatory wave and the expected time required for an approaching depolarization wave to travel from this site to the EB origin. The latter was determined by dividing the distance from the last activated electrode to the EB origin by the median conduction velocity (4.5mm/ 0.55 mm/ms ~ 8 ms). The degree of pre-excitation was then estimated by calculating the difference between the local activation time at the EB origin and the expected activation time (20 – (32+8 = 40) = -20 ms).

To study the impact of an EB on the complexity of the fibrillatory process in the epicardial plane, the incidence of conduction block at every EB origin was determined. Therefore, the conduction time to each of the 8 surrounding electrodes of an EB origin was calculated. Conduction block was defined as an inter-electrode conduction time of > 30 ms. This corresponded with a conduction velocity of < 7.5 cm/s.

Statistical Analysis

All data are expressed as mean ± standard deviation. Pearson's correlation coefficient (r) and independent student's T-tests were used to validate the significance of the acquired results. A probability level of 5% was considered statistically significant.

Results

Incidence of Epicardial Breakthroughs

Examples of EB (*) observed at the right atrial free wall are demonstrated in the isochronal maps in Figure 2. The first map in the upper panel shows a single fibrillatory wave propagating without any conduction disturbances. Before the next entering fibrillatory wave could activate the mapping area, there was premature activation of atrial tissue by an EB (second map). The first map in the middle panel shows again a fibrillatory wave

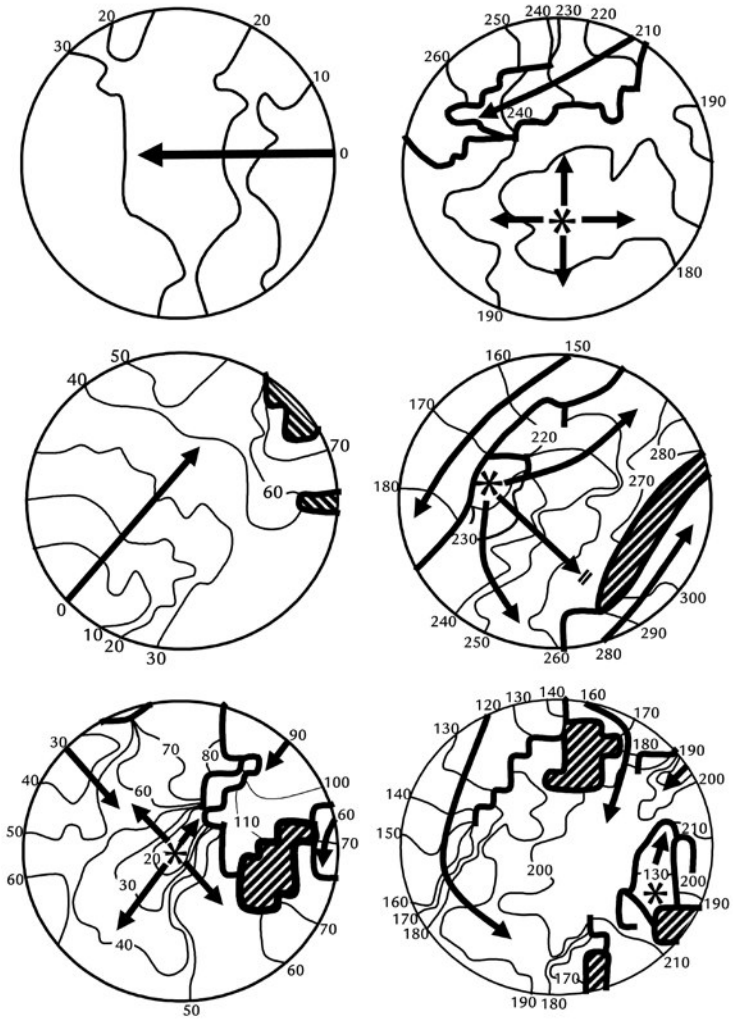

Figure 2.

Isochronal maps of the right atrial free wall demonstrating typical examples of EB observed during AF. Isochronal maps were drawn at 10 or 20 ms intervals, arrows indicate main direction of activation, lines of conduction block are represented by thick black lines and the origin of an EB is indicated with an asterix.

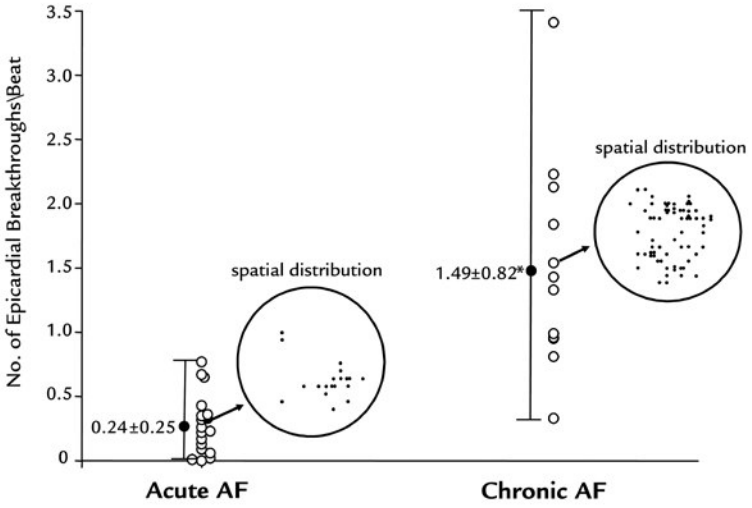

Figure 3.

The incidence of EB observed within an area of 3.6X3.6 cm at the right atrial free wall in each AAF and CAF patient (white circles); the incidence of EB during CAF was significantly higher than during AAF. The spatial distribution of EB in the mapping area (black circles) is shown for one representative AAF and CAF patient. EB were found scattered throughout the entire mapping area and there appeared to be no predilection sites for EB within 8 seconds of AF. * p<0.001

activating the entire mapping area. In the following beat, the next entering fibrillatory wave activates only a small part of the mapping area due to presence of a long line of conduction block (thick black line). There was no wavefront propagating in the epicardial plane which activated atrial tissue at the other site of the line of conduction block. Instead, this area was now activated by an EB.

In the first map in the lower panel, the mapping area is activated by an EB and multiple wavelets propagating in the epicardial plane. However, these wavelets fail to elicit a response in a small part of the mapping area resulting in an island of intra-atrial conduction block (shaded area). Then an EB emerges within this island of intra-atrial conduction block and propagates over a small distance before it encounters atrial tissue which is still refractory.

A total number of 257 and 551 EB were observed during respectively AAF and CAF. The incidence of epicardial breakthrough in the CAF patients was higher than in the AAF patients (1.49 ± 0.82 [0.33-3.41]/beat versus 0.24 ± 0.25 [0-0.77]/beat, p<0.001, **Figure 3**). In CAF patients, EB arose more frequently from islands of intra-atrial conduction block than in AAF patients (13% versus 4%, p< 0.001). In the AAF and CAF patients, a higher incidence of EB was associated with a lower conduction velocity (AAF: r = -0.58, p = 0.007, CAF: r = -0.78, p = 0.003). There was no relation between the incidence of EB and the median AFCL or left atrial size.

The spatial distribution of EB for a typical AAF and CAF patient is also shown in **Figure 3**. EB were scattered throughout the mapping area and no predilection sites could be identified. In patients with a relative low incidence of EB, there seemed to be some clustering of breakthrough sites in the mapping area, suggesting predilection sites for EB to occur. However, with an increasing incidence of EB, EB emerged more diffusely throughout the mapping area suggesting that the apparent predilection sites for EB were in fact due to the low incidence.

EB origin of 20 consecutive EB in one CAF patient are shown in **Figure 4**; each EB is marked with an asterix. Sites which were previously activated by an EB are marked with a black circle. These maps show a clear shift in the origin of consecutive EB.

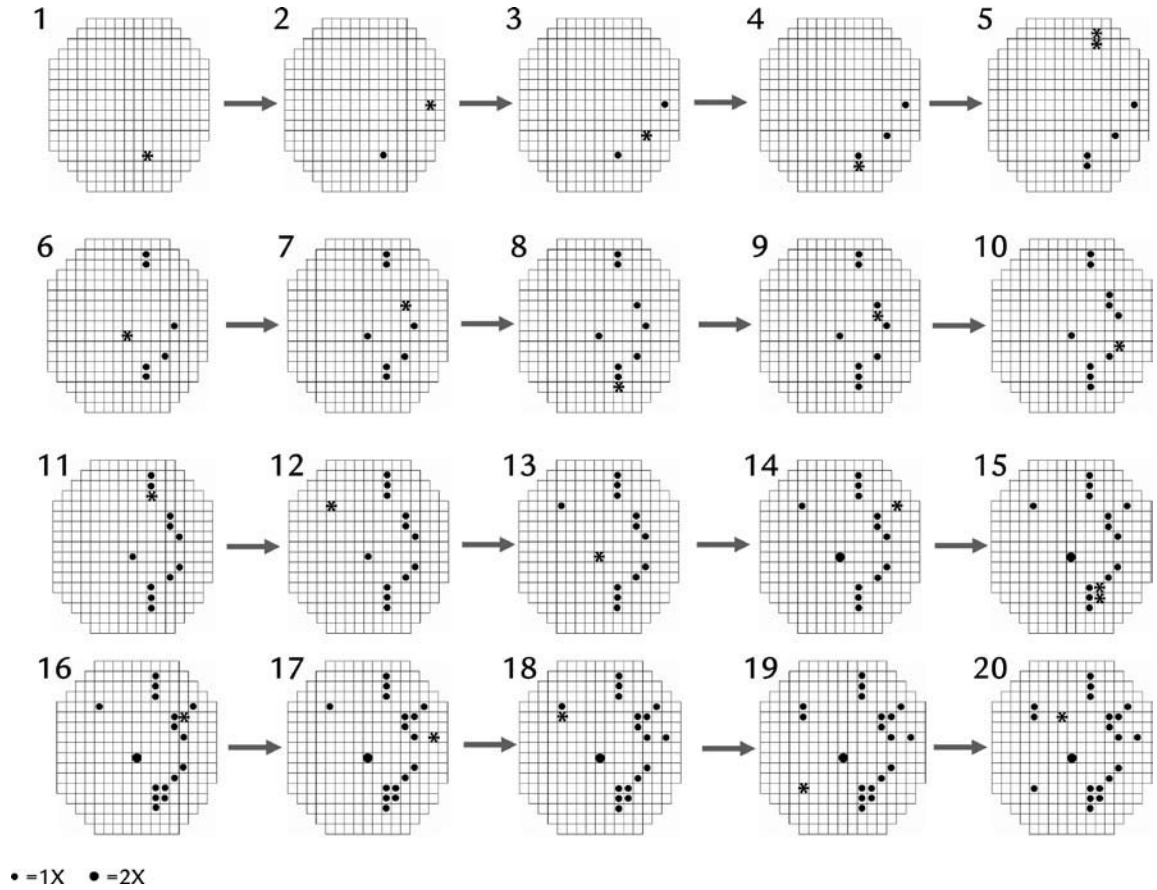

Figure 4.
Location of EB origin of 20 consecutive EB in one CAF patient; each EB is marked with an asterix. Sites which were previously activated by an EB are marked with a black circle. These maps show a clear shift in the EB origin of consecutive EB.

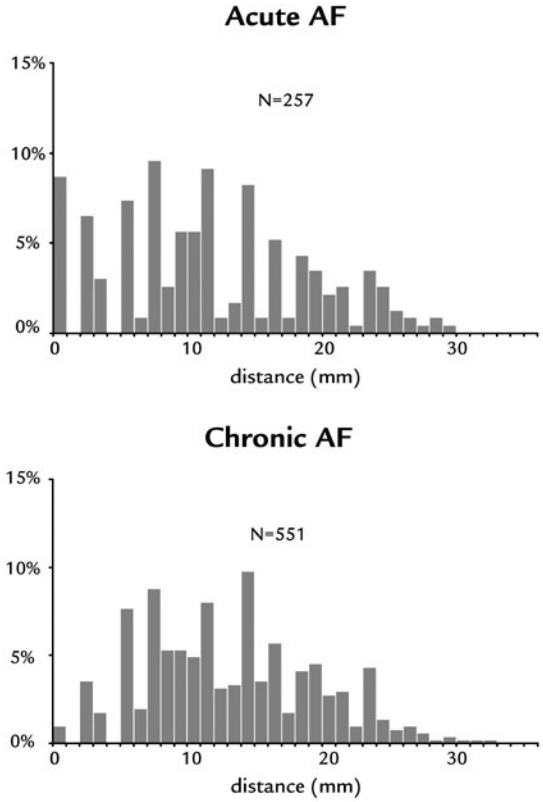

Figure 5.
Relative frequency distribution of distances between consecutive EB during AAF and CAF. There was no difference in the averaged distance between consecutive EB in AAF patients and CAF patients (AAF: 10 ± 3 (0-29) mm, CAF: 12 ± 2 (0-32) mm, p = 0.3).
mm = milliseconds.

The area of earliest activation sometimes covered more than one electrode (5th and 15th EB). Distances between consecutive EB during AAF and CAF are shown in **Figure 5**. The averaged distance between consecutive EB in AAF patients did not differ from CAF patients (AAF: 10 ± 3 (0-29) mm, CAF: 12 ± 2 (0-32) mm, p = 0.3). Median time between consecutive EB in the CAF patients was shorter than in the AAF patients (CAF: 2000 ± 1145 ms, AAF: 4349 ± 3807 ms, p = 0.01).

Electrogram Characteristics at the Site of Epicardial Breakthrough

In the AAF and CAF patients, respectively 42 ± 31% and 38 ± 18% of the breakthrough electrograms were single potentials (p = 0.1). The median RS difference of single potentials recorded at the EB site was -0.17 (P5: -0.07, P95: -0.46) during AAF and -0.09 (P5: -0.67, P95: 0.17) during CAF, indicating the presence of a R wave preceding the negative deflection. The majority of electrograms recorded at the EB origin consisted of double

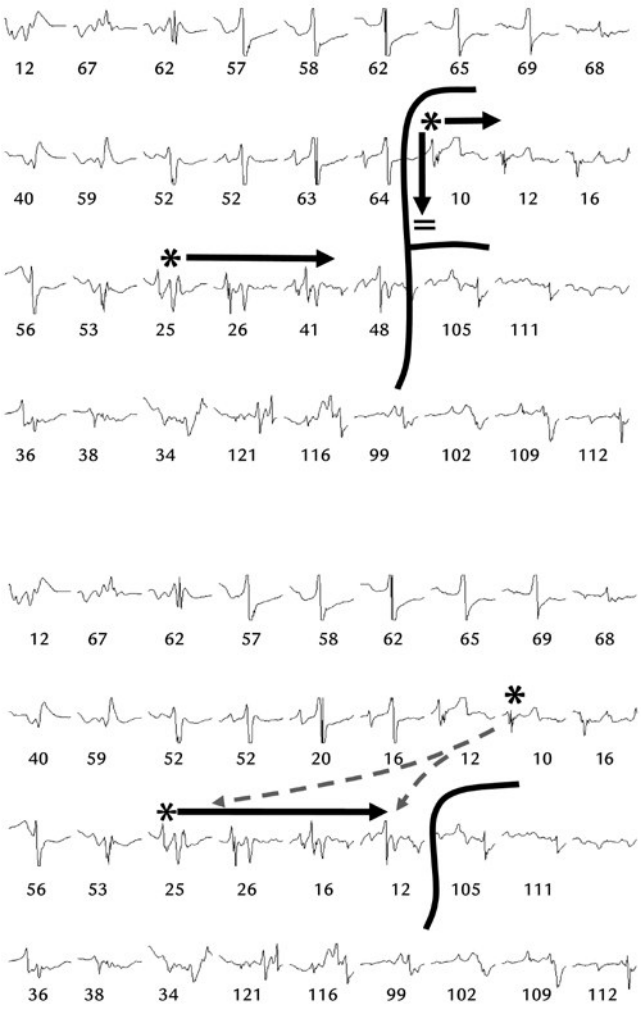

Figure 6.

Electrograms recorded at the right atrial free wall during CAF.
Top: the maximum negative derivative of unipolar fibrillation potentials was marked, revealing 2 EB (*, activation time 10 and 25 ms). *Bottom:* local activation times are determined by marking smaller components preceding the components with the steepest negative deflection. Now, the wavefront seems to propagate from the first EB to the second EB site. The second EB could therefore be the result of conduction of a wavefront from the first EB site through deeper layers of the myocardium.

and fractionated potentials (AAF: 64 ± 32%, CAF: 62 ± 18%). During AAF and CAF, the presence of double and fractionated potentials at the EB origin was inversely related with the EB interval (AAF: r = -0.14, p = 0.04, CAF: r = -0.10, p = 0.04).

Figure 6 shows electrograms recorded in a small part of the mapping area (18x6.75 mm). In the upper panel, local activation times at each electrode were determined by marking the maximum negative derivative of unipolar fibrillation potentials. At t = 10 ms, an EB

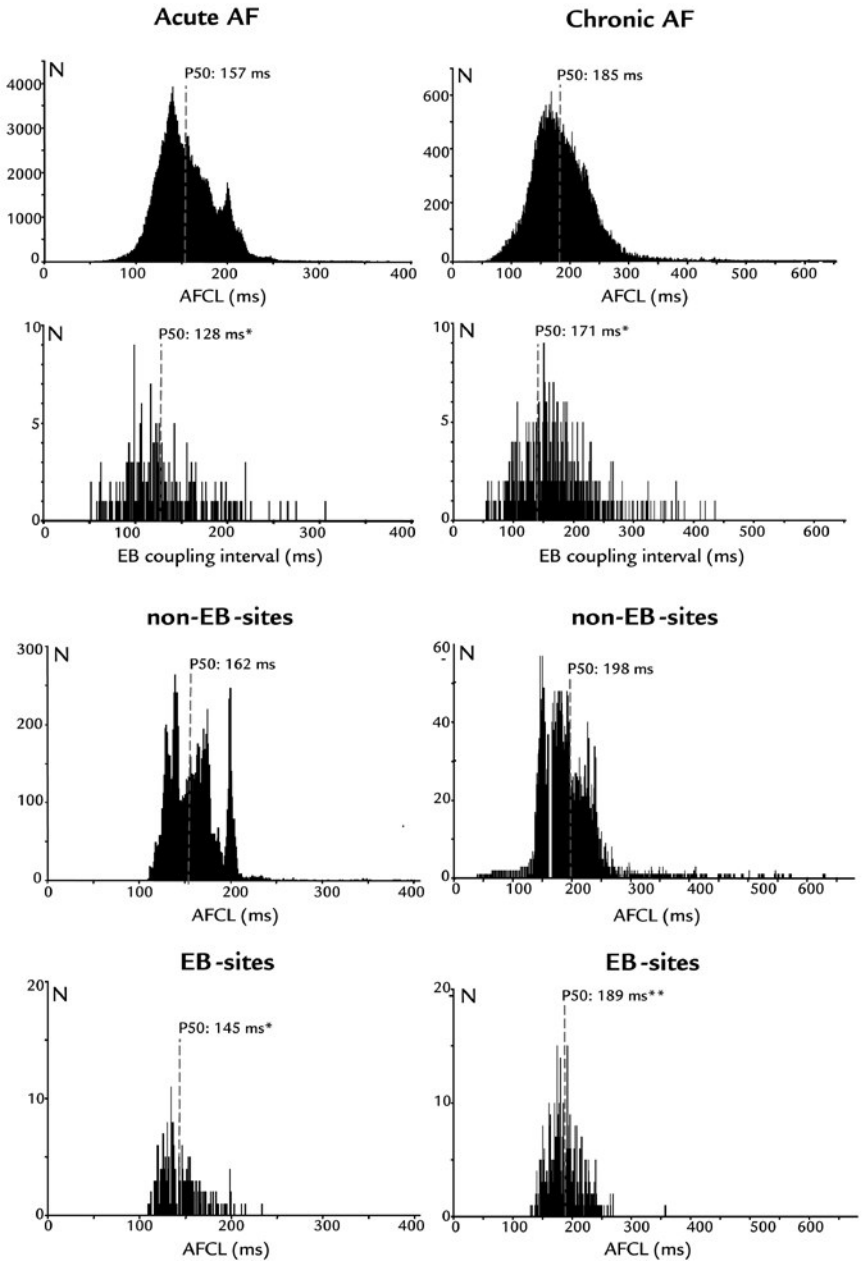

Figure 7.

Top: Interval histograms demonstrating all fibrillation intervals and EB coupling intervals during AAF and CAF. In the AAF and CAF patients, EB coupling intervals (AAF: 128 ± 27 ms CAF: 171 ± 26 ms) were significantly shorter than the median AF cycle length (AAF: 157 ± 26 ms CAF: 185 ± 28 ms). *Bottom:* relative frequency distribution of median AFCL at EB sites and sites at which EB were never observed. During both AAF and CAF, the median AFCL at EB sites was shorter than at non-EB sites (AAF: 145 ± 23 ms versus 162 ± 48 ms, CAF: 189 ± 29 ms versus 198 ± 80 ms). *p<0.01, **p = 0.02

occurred (*) which blocked downwards and to the left side. Another EB emerged (t = 25 ms) at a distance of 9 mm from the first EB. In the lower panel, local activation times are determined by marking smaller components preceding the components with the steepest negative deflection. The wavefront originating from the first EB site seems to propagated to the second EB site. These recordings suggest that the second EB could be explained by conduction of a wavefront from the first EB site through deeper layers of the myocardium, giving rise to far-field potentials in the epicardial electrograms.

Impact of Epicardial Breakthrough on Atrial Fibrillation
Premature Activation

The interval histograms in the upper panel of Figure 7 give all fibrillation intervals recorded in the entire mapping area during AAF (left, n = 224,615) and CAF (right, n = 60,609). The averaged median AFCL at the right atrial free wall in the AAF patients ranged between 122 and 215 [157 ± 26] ms and in the CAF patients between 149 and 233 [185 ± 28] ms. As previously reported, the AFCL during CAF was longer than during AAF (p = 0.025).

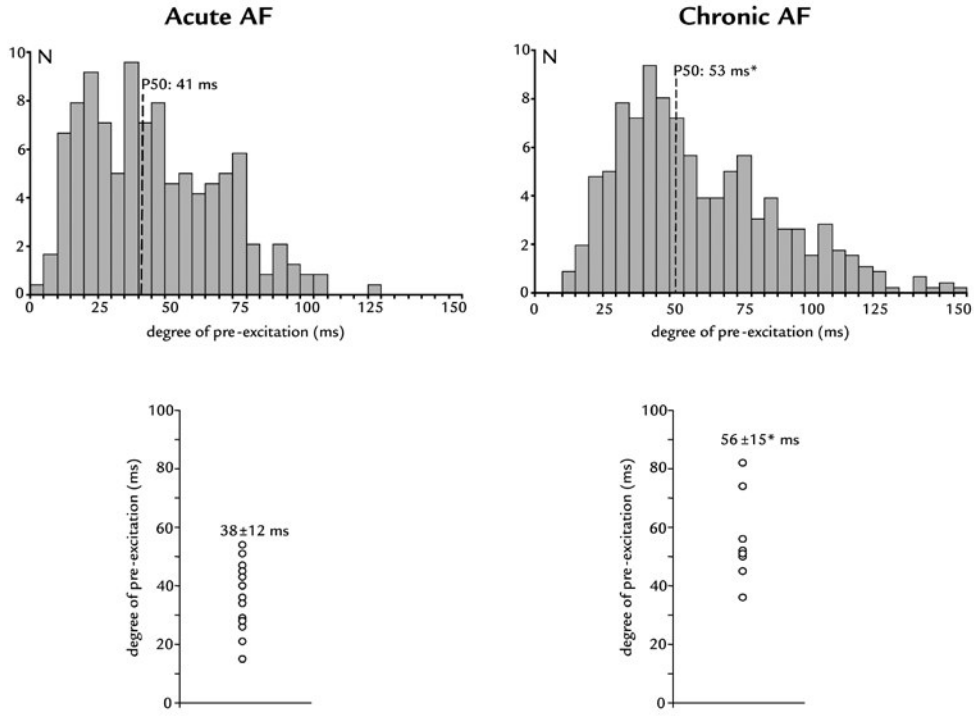

Figure 8
Top: the degree of pre-excitation by all EB during AAF and CAF. *Bottom:* the median degree of pre-excitation for each AAF and CAF patient separately. * p<0.001

As expected, histograms of the EB coupling intervals show that EB coupling intervals were significantly shorter than the median AF cycle length (AAF: 128 ± 27 ms, CAF: 171 ± 26 ms, $p<0.01$). The longest EB coupling intervals were the result of EB emerging from islands of intra-atrial conduction block. The lower panel shows the frequency distribution of the median AFCL at EB and non-EB sites. During both AAF and CAF, the median AFCL at EB sites was shorter than at non-EB sites (AAF: 145 ± 23 ms versus 162 ± 48 ms, $p<0.001$, CAF: 189 ± 29 ms versus 198 ± 80 ms, $p = 0.02$).

Degree of Pre-excitation

The degree of pre-excitation by EB during AAF and CAF is shown in the upper panel of Figure 8. The lower panel shows the degree of pre-excitation for each AAF and CAF patient individually. The degree of pre-excitation by EB in the CAF patients was higher than in the AAF patients (CAF: 56 ± 15 ms versus AAF: 38 ± 12 ms, $p<0.001$).

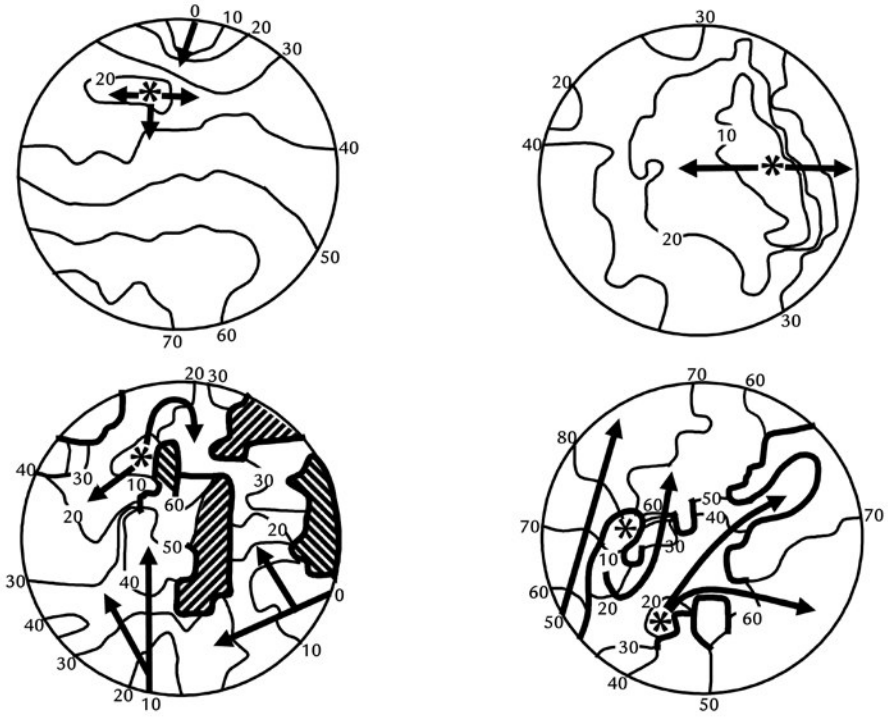

Figure 9.
Isochronal maps of the right atrial free wall demonstrating EB with variable degrees of expansion. Isochronal maps were drawn at 10 or 20 ms intervals, arrows indicate main direction of activation, lines of conduction block are represented by thick black lines and the origin of an EB is indicated with an asterix.
See text for further explanation.

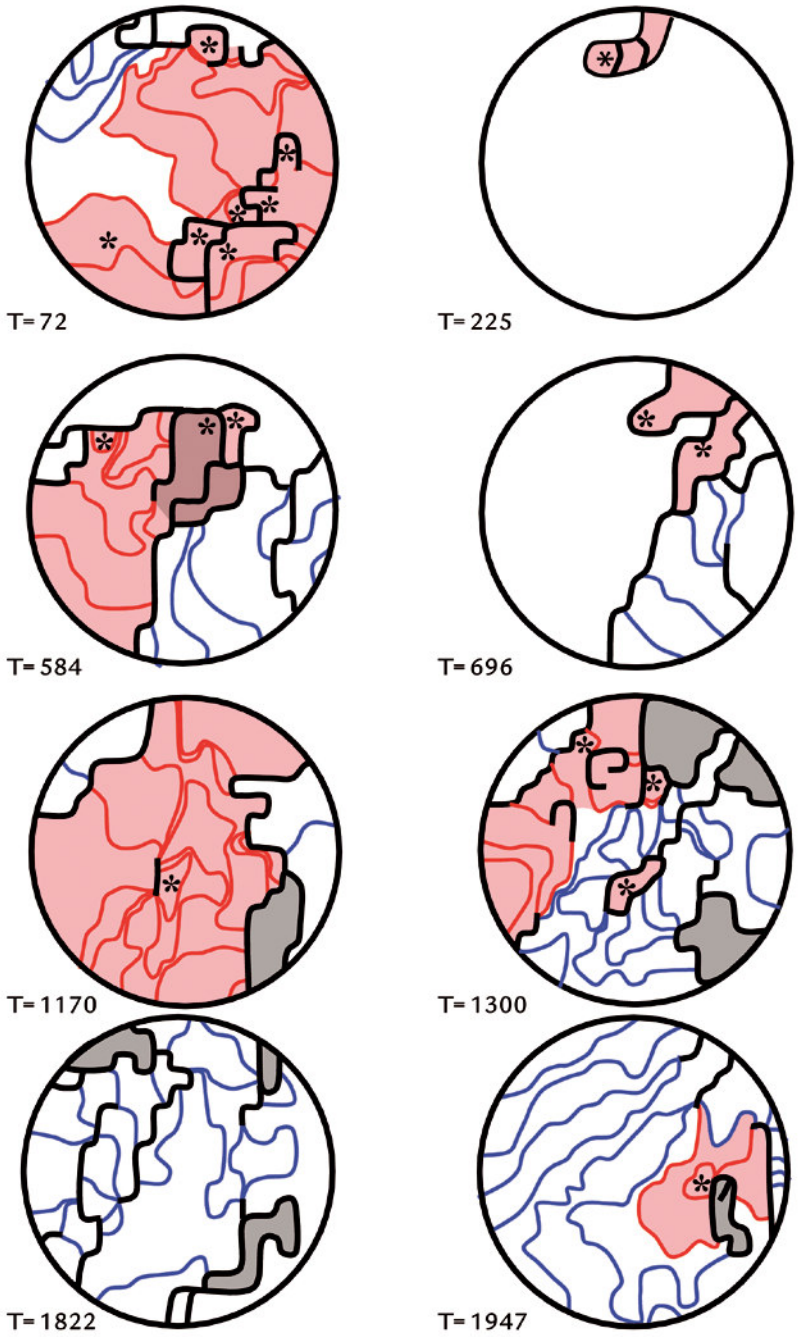

Figure 10.

Sixteen consecutive isochronal maps of the right atrial free wall obtained from a CAF patient. EB sites are marked with an asterix. Red colored areas represent parts of the mapping area activated by EB, the remaining part which is activated by epicardial waves is indicated by blue isochrones.

T= 429
T= 942
T= 1675
T= 2250
T= 254
T= 804
T= 1475
T= 2118

Expansion of Epicardial Breakthrough

Isochronal maps of the right atrial free wall in Figure 9 show examples of EB (*) observed during AF. Expansion of the wavefront from its epicardial origin occurred in a variable degree. The upper left map shows a new wavefront arising in the upper part of the mapping area which fused with a passing fibrillatory wave. This EB wave merely resulted in a 'local reset' and the complexity of the activation pattern at this site was not affected. The second map shows an EB which activated almost the entire mapping area.

An example of conduction block of the breakthrough wavefront immediately at the site of origin is demonstrated in the lower left panel. Part of the new wavefront turned around an area of conduction block and propagated downward over a small distance before it encountered again an area of conduction block. Expansion of the EB in other directions was also limited by areas of conduction block or by fusion with other fibrillatory waves.

An example of multiple EB appearing in close proximity to each other is shown in the lower right map. Again, expansion of these two EB is hampered by either fusion with other fibrillatory waves or by the occurrence of conduction block. From the maps in the lower panel it is clear that EB may considerably enhance the complexity of epicardial activation.

The incidence of conduction block at the EB origin in at least one direction was 52 ± 35% during AAF and 74 ± 21% during CAF. In all other cases, there was either a radial spread of the EB or fusion with other fibrillatory waves. Incidence of conduction block was associated with shorter EB couplings intervals (AAF: no conduction block: EB coupling intervals 144 ± 41 ms, conduction block: 137 ± 52, $p = 0.01$; CAF: no conduction block: EB coupling intervals 186 ± 90 ms, conduction block: 168 ± 62, $p = 0.01$).

Figure 10 shows sixteen consecutive isochronal maps of the right atrial free wall obtained from a CAF patient. The EB sites are marked with an asterix. Red colored areas represent parts of the mapping area activated by EB, the remaining part which is activated by epicardial waves is indicated by blue isochrones. EB frequently occurred in this patient, it was absent during only one 'beat'. There is a considerable shift in the origin of consecutive EB. Expansion of EB from the site of origin was variable, ranging from only 2.25 mm (last map) to the entire mapping area (36 mm, third map). In the majority of the EB, expansion was hampered by conduction block of the wavefront at the EB origin.

Discussion

This study demonstrated that EB frequently occur at the right atrial free wall in humans with AF. These EB were solitary events scattered throughout the mapping area. The high incidence of conduction block at the EB origin combined with the variable expansion of EB due to fusion with other fibrillatory waves or areas of conduction block enhanced the complexity of patterns of activation in the epicardial plane. Comparing AAF and CAF patients, EB occurred more frequently during CAF with a higher degree of local pre-excitation.

2-Dimensional versus 3-Dimensional Conduction

Experimental studies demonstrated that EB are the result of conduction from the endocardial to the epicardial layer. [2;3] We therefore assumed that de novo appearing waves at the epicardium observed during AF in humans are also due to transmural conduction of fibrillatory waves. Breakthrough of a wavefront in the epicardial plane can only occur when activation of the endocardial and epicardial layer is dissociated and when an 'excitable gap' is present which allows an intramural wavefront to arise at the epicardium. Theoretically, an epicardial breakthrough is more likely to occur when the diastolic interval is prolonged. Prolongation of the diastolic interval during AF can be due to 1) shortening of the action potential duration, 2) an increase in pathlength of fibrillatory waves due to lines of conduction block and 3) slowing of conduction.

A lower conduction velocity was related to a higher incidence of EB. Comparing the incidence of EB between AAF patients and CAF patients, EB occurred more frequently during CAF. Long-standing AF is associated with shortening of the refractory period, a decrease in conduction velocity and a higher incidence of conduction block.[8] These electrical alterations result in lengthening of the diastolic interval thereby increasing the chance for endocardial fibrillatory waves to emerge on the epicardial surface. Simultaneous mapping of adjacent epicardial and endocardial layers in isolated canine atria demonstrated that the subepicardial layer leads the activation of the atrial wall during both sinus rhythm and atrial pacing.[3] In a recent study, we proposed that the thin subepicardial layer also plays a leading role in propagation of fibrillatory waves.[7]

We hypothesized that the thin subepicardial layer is damaged in patients with CAF, due to e.g. fibro-fatty replacement.[9] It is likely that injury of this subepicardial layer causes dissociation in activation of the endo- and epicardial layer. Patterns of activations are now determined by the architecture of the atrial wall and fibrillatory waves may emerge at the epicardium through the complex network of the pectinate muscles. This mechanism could account for the diffuse distribution of EB and the wide variety of EB coupling intervals found in this study.

RS–differences of the single potentials recorded at breakthrough sites indicate that the negative deflection is preceded by R waves of variable amplitudes. The R waves could be explained by intramural wavefronts propagating towards the breakthrough sites. The

large number of fractionated potentials recorded at the EB origin is due to the high incidence of conduction block at these sites. Conduction block is more likely to occur at shorter EB coupling intervals. At shorter coupling intervals, the EB wavefront encounters atrial tissue which is still refractory and hence, conduction of the expanding wavefront is blocked.

The present study also showed that the degree of pre-excitation of atrial tissue by EB during CAF is larger than during AAF. The degree of pre-excitation found in this study suggests that there is an asynchronous activation of the endocardial and epicardial layer. Animal studies have demonstrated that dissociation in conduction between adjacent endocardial and epicardial layer exists, particularly in thicker parts of the atria like the area of the pectinate muscles.[3] In this case, asynchronous activation of the endocardium and epicardium could be caused by a transmural angle of a fibrillatory wave which results in early activation of the endocardium relative to the epicardium (lower left panel Figure 11). Otherwise, there could also be complete transmural dissociation in conduction during which the endocardium and epicardium are completely activated independently from each other (lower right panel Figure 11). In the CAF group, dissociation in conduction between the endocardial and epicardial layer could be enhanced by alterations of the myocardial structure such as increased interstitial fibrosis.

Impact of Epicardial Breakthroughs

EB resulted in local shortening of the atrial fibrillation cycle length. We rarely observed a centrifugal spread of the wavefront from the site of earliest epicardial activation capturing the entire mapping area. In the majority of the cases, expansion of the breakthrough wavefront was limited by fusion with other fibrillatory waves or by encountering areas of conduction block. Also, repetitive focal patterns of activation were never found. Comparing AAF and CAF patients, CAF patients have a longer median AFCL and a higher incidence of EB. As EB shorten AFCL, AFCL would have been even longer if there had been no EB. Hence, EB give rise to focal activity without being a focal source.

Focal Activity

De novo appearing waves at the atrial surface can be also caused by enhanced automaticity, triggered activity or micro-reentry. In diseased atria, stretch and ischemia increase the probability for focal activity to develop. [10]

A micro-reentry circuit in the *epicardial* plane giving rise to new fibrillatory waves is unlikely; the size of the reentry circuit should then have been smaller than the spatial resolution of the mapping array used (2.25 mm) to be undetected and this would require extreme low conduction velocities.

In case of a stationary source giving rise to de novo appearing waves, one would expect that the wavefront originates from the same site for at least in more than one beat with small variations in coupling intervals at the site of earliest activation.

However, our data showed that there is a considerable shift in the origin of de novo appearing waves and that these new waves appear at multiple sites throughout the mapping area with a wide variety in coupling intervals. Also, repetitive focal patterns of activation emerging from a breakthrough site were never observed. In case of focal activity, the new arising wavefronts in the epicardial plane observed in our study could only be explained by multiple, wandering foci with an irregular rate.

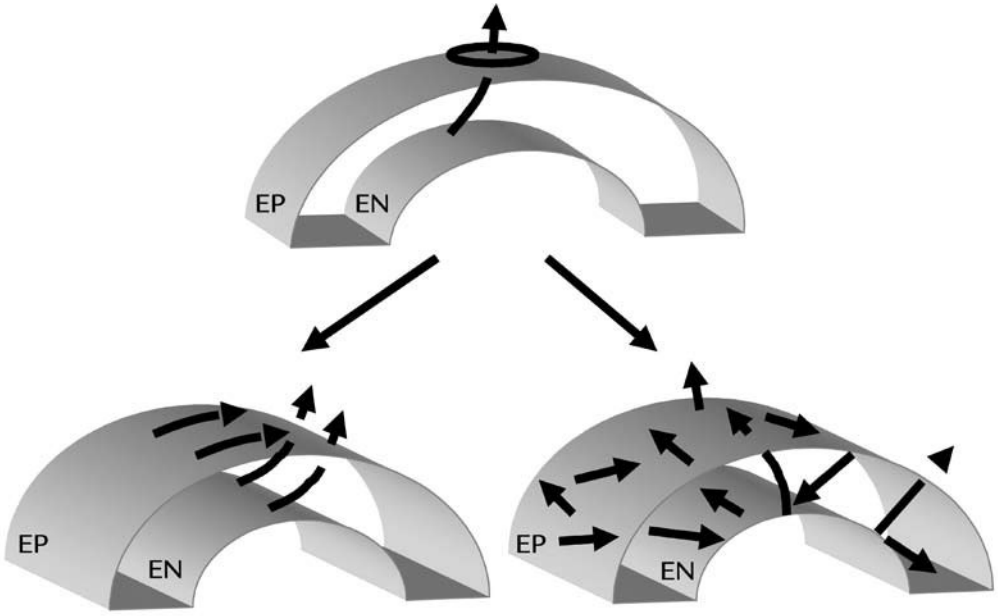

Figure 11.
De novo emerging fibrillatory waves observed in this study are most likely the result of transmural propagation of epicardial breakthrough of fibrillatory waves. This findings implies that fibrillatory waves either have a transmural angle resulting in an endo- to epicardial activation direction (lower left panel) or that there is a complete dissociation in activation between the endocardial and epicardial layer (lower right panel).
EN = endocardium, EP = epicardium.

Study Limitations

All our measurements were made during open chest surgery and could therefore be affected by the anesthetic drugs used. As this is the case for both AAF and CAF patients, comparison of EB observed between these two groups seems to be justified.

As we did not perform simultaneous mapping of the endocardium and epicardium layer, comments on the underlying mechanism of the observed EB can only be based on indirect evidence. Also, high density mapping was limited to the right atrial free wall. Further research will be needed to investigate occurrences of EB at other sites in the atria and to unravel the underlying mechanism of this phenomena.

Clinical Implications

In patients with CAF there is a higher incidence of EB compared to AAF patients, suggesting that transition from AAF to CAF is associated with progression from 2-dimensional conduction to 3-dimensional conduction of fibrillatory waves. When there is a transmural propagation of fibrillatory waves, the atria can contain more wavelets, thereby stabilizing AF.

Several intra-operative, epicardial multi-site mapping studies of CAF performed in patients with valvular disease revealed focal patterns of activation originating from circumscribed areas in the left atrium.[11-13] These activation patterns were thought to be the result of the presence of high frequency sources giving rise to fibrillatory conduction and ablation of these sources would subsequently abolish AF. However, as the results of our study are supportive for transmural conduction of fibrillatory waves giving rise to new wavefronts emerging at the epicardial plane, ablation of such areas would not be effective in eliminating AF.

Conclusions

The results of this study are most consistent with transmural propagation of fibrillatory waves. In humans with AF, EB frequently occur at the right atrial free wall. EB appear as solitary events scattered throughout the mapping area and were preceded by a wide variety of fibrillation intervals. At the site of origin, there was a high incidence of conduction block, enhancing the complexity of patterns of activation in the epicardial plane. Expansion of EB was variable due to fusion with other fibrillatory waves and areas of conduction block. Comparing AAF and CAF patients, EB occurred more frequently during CAF with a higher degree of local pre-excitation. These findings support the hypothesis of electropathological alterations in the thin subepicardial layer leading propagation of fibrillatory waves in patients with CAF.

References

1. Derakhchan K, Li D, Courtemanche M et al. Method for simultaneous epicardial and endocardial mapping of in vivo canine heart: application to atrial conduction properties and arrhythmia mechanisms. J Cardiovasc Electrophysiol. 2001;12:548-555.
2. Gray RA, Pertsov AM, Jalife J. Incomplete reentry and epicardial breakthrough patterns during atrial fibrillation in the sheep heart. Circulation. 1996;94:2649-2661.
3. Schuessler RB, Kawamoto T, Hand DE et al. Simultaneous epicardial and endocardial activation sequence mapping in the isolated canine right atrium. Circulation. 1993;88:250-263.
4. Wu TJ, Yashima M, Xie F et al. Role of pectinate muscle bundles in the generation and maintenance of intra-atrial reentry: potential implications for the mechanism of conversion between atrial fibrillation and atrial flutter. Circ Res. 1998;83:448-462.
5. Konings KT, Kirchhof CJ, Smeets JR et al. High-density mapping of electrically induced atrial fibrillation in humans. Circulation. 1994;89:1665-1680.
6. Holm M, Johansson R, Brandt J et al. Epicardial right atrial free wall mapping in chronic atrial fibrillation. Documentation of repetitive activation with a focal spread – a hitherto unrecognised phenomenon in man. Eur Heart J. 1997;18:290-310.
7. Houben R, de Groot NM, Smeets JLRM, Becker AE, LindemansFW, Allessie MA. S-wave predominance of epicardial electrograms during atrial fibrillation in humans: Indirect evidence for a role of the thin subepicardial layer. Heart Rhythm 1, 639-647.
8. Wijffels MC, Kirchhof CJ, Dorland R et al. Atrial fibrillation begets atrial fibrillation. A study in awake chronically instrumented goats. Circulation. 1995;92:1954-1968.
9. Becker AE. How structurally normal are human atria in patients with atrial fibrillation ? Heart Rhythm 1, 627-631.
10. Chen SA, Chiang CE, Yang CJ et al. Sustained atrial tachycardia in adult patients. Electrophysiological characteristics, pharmacological response, possible mechanisms, and effects of radiofrequency ablation. Circulation. 1994;90:1262-1278.
11. Harada A, Sasaki K, Fukushima T et al. Atrial activation during chronic atrial fibrillation in patients with isolated mitral valve disease. Ann Thorac Surg. 1996;61:104-111.
12. Harada A, Konishi T, Fukata M et al. Intraoperative map guided operation for atrial fibrillation due to mitral valve disease. Ann Thorac Surg. 2000;69:446-450.
13. Nitta T, Ishii Y, Miyagi Y et al. Concurrent multiple left atrial focal activations with fibrillatory conduction and right atrial focal or reentrant activation as the mechanism in atrial fibrillation. J Thorac Cardiovasc Surg. 2004;127:770-778.